



Title	Optical selection of a multiple phase order in the charge density wave condensate o-TaS3 using a spectrally resolved nonequilibrium measurement
Author(s)	Toda, Y.; Onozaki, R.; Tsubota, M.; Inagaki, K.; Tanda, S.
Citation	Physical Review B, 80(12), 121103 <a href="https://doi.org/10.1103/PhysRevB.80.121103">https://doi.org/10.1103/PhysRevB.80.121103</a>
Issue Date	2009-09
Doc URL	<a href="http://hdl.handle.net/2115/39541">http://hdl.handle.net/2115/39541</a>
Rights	©2009 The American Physical Society
Type	article
File Information	PRB80-12_121103.pdf



[Instructions for use](#)

# Optical selection of a multiple phase order in the charge density wave condensate $o$ -TaS<sub>3</sub> using a spectrally resolved nonequilibrium measurement

Y. Toda, R. Onozaki, M. Tsubota, K. Inagaki, and S. Tanda

Department of Applied Physics, Hokkaido University, Kita 13 Nishi 8 Kita-ku, Sapporo 060-8628, Japan

(Received 6 June 2009; revised manuscript received 9 August 2009; published 28 September 2009)

We investigate the spectrally resolved transient reflectivity changes  $\Delta R(T, \tau, \lambda)$  in the charge density wave (CDW) conductor  $o$ -TaS<sub>3</sub>. A distinct near-infrared resonance in this compound emphasizes the characteristic  $\Delta R(\lambda)$  resonances, and allows a selection of coexisting CDW phases with different nonequilibrium carrier dynamics. Furthermore, the spectrally resolved  $\Delta R(\tau)$  characterizes the collective oscillations associated with the individual states. We believe that this demonstration paves the way for the optical selection of the multiphase order that plays an important role in various macroscopic quantum systems.

DOI: [10.1103/PhysRevB.80.121103](https://doi.org/10.1103/PhysRevB.80.121103)

PACS number(s): 71.30.+h, 71.45.Lr, 74.25.Gz, 78.47.J-

## I. INTRODUCTION

The coexistence of several ordered electronic states has played an important role in various macroscopic quantum systems such as high- $T_c$  superconductors and charge density wave (CDW) conductors. Of the various spectroscopic approaches, optical time-resolved spectroscopy is a unique method that probes phase ordering via nonequilibrium carrier relaxation.<sup>1-3</sup> For multiple ground systems, a selective evaluation of the individual states can be realized by determining the difference between the associated relaxation components with high time resolution.<sup>4-6</sup> Selective enhancement of the signals from the individual states has also been demonstrated by changing the resonant conditions for the higher excited states.<sup>6,7</sup> However, the complexity of the electronic states in those materials requires more comprehensive approach which emphasizes the selectivity.

In this Rapid Communication, we demonstrate an optical selection of the multiphase order in  $o$ -TaS<sub>3</sub> using a spectrally resolved pump-probe measurement. Owing to the well-defined excited resonance in this compound, pronounced reflectivity changes  $\Delta R$  are observed in both the spectral and temporal domains across the characteristic temperatures, and can be identified as responses originating from the two types of CDW phases. This identification is also supported by the coherent oscillations whose spectral and temperature dependences highlight the phase transition in each state.

$o$ -TaS<sub>3</sub> is one of the most widely studied quasi-one-dimensional (1D) compounds that undergoes phase transitions associated with the formation of three-dimensionally (3D) ordered CDWs.<sup>8-20</sup> Below the phase-transition temperature ( $T_{CDW}$ ), a Peierls gap opens at the Fermi level, resulting in a change of the conductivity from metallic to semiconducting. At lower temperatures than  $T_{CDW}/2$ , several remarkable changes occur; a deviation from the activation law in linear conductivity, and the appearances of the second threshold, subgap structure, and new resonance, respectively, in nonlinear conductivity,<sup>9</sup> tunneling spectroscopy,<sup>17</sup> and dielectric spectroscopy.<sup>11-13,18</sup> In the similar temperature region, a splitting of satellite peak was also observed in a synchrotron x-ray measurement,<sup>19</sup> suggesting a coexistence of different CDW phases. The dielectric measurement provides evidence of two glass transitions at  $T \sim 40$  and  $\sim 10$  K.<sup>11-15</sup>

## II. EXPERIMENTAL

High quality samples with a length of a few mm (along the conducting axis) and several tens of  $\mu\text{m}$  wide were grown with a chemical vapor transport technique. Note that we measured several samples and obtained similar results as reported below. This compound has two different types of crystal structure, namely an orthorhombic structure ( $o$ -TaS<sub>3</sub>) and a monoclinic structure ( $m$ -TaS<sub>3</sub>); the former exhibits only one 3D CDW phase transition at  $T_{CDW}=220$  K while the latter exhibits two independent phase transitions at  $T_{CDW}=240$  and 160 K. The resistivity measurements of the samples show that the metallic conductivity at room temperature becomes semiconducting below  $T=220$  K, indicating an  $o$ -TaS<sub>3</sub> crystal. This assignment is also supported by the near-infrared optical reflection spectra [Fig. 1(a)], in which a distinct peak around  $\lambda=900$  nm is in good agreement with a previous report on  $o$ -TaS<sub>3</sub>.<sup>10</sup>

For the measurement, we employed a two-color pump and probe approach, in which the coaxial configuration between the pump and probe beams allows the excitation of crystals with small sizes.<sup>6</sup> Ultrafast photoexcitation was realized us-

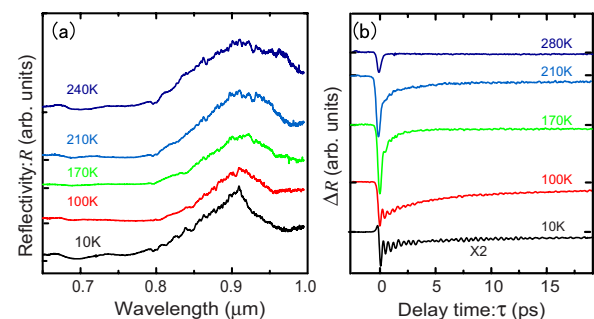


FIG. 1. (Color online) (a) Optical reflectivity  $R(\lambda)$  around an interband resonance of  $o$ -TaS<sub>3</sub> at various temperatures. The incident laser polarization was set parallel to the chain axis (conducting axis). (b) A typical series of transient reflectivity changes,  $\Delta R(\tau)$ , at various temperatures. The  $\Delta R$  obtained at  $\lambda_{pr}=880$  nm showing a decrease in  $R$  from its equilibrium value is selected to make it easy to compare results obtained below and above the CDW transition temperature ( $T_{CDW}=220$  K). The pump and probe polarizations were parallel to the conducting axis.

ing a mode-locked 100 fs Ti-sapphire laser oscillator operating at a repetition rate of about 76 MHz, which synchronously pumped an optical parametric oscillator (OPO). The probe beam was extracted from the fundamental ( $\lambda_{pr}=700\text{--}900\text{ nm}$ ) with a spectral width of  $5\text{--}10\text{ nm}$ , and the pump beam was delivered by the OPO ( $\lambda_{pm}=1060\text{--}1260\text{ nm}$ ). To avoid contributions from the higher excited states, a probe beam energy is selected that exceeds that of the pump beam. The cross correlation between the pump and probe pulses in a nonlinear optical crystal exhibited a temporal resolution of 200 fs. The pump and probe pulse polarizations were parallel to the conducting axis because  $\Delta R$  is dominant in this direction. The total fluence was kept lower than  $50\ \mu\text{J}/\text{cm}^2$ , and the pump/probe ratio was 2:1. To measure the transient response, the pump pulse was mechanically delayed with respect to the probe pulses using a translation stage. The reflectivity change  $\Delta R$  in the probe was detected with a lock-in amplifier. A spectrally resolved investigation was achieved by scanning the wavelength of the probe by tuning the birefringence filter of the oscillator with  $\delta\lambda=5\text{ nm}$ . We checked that  $\Delta R$  was almost independent of the pump wavelength by comparing it with the  $\Delta R$  signal that we obtained using the second harmonic of the pump pulse. In this way, we obtained  $\Delta R$  as a function of temperature, delay time and probe wavelength:  $\Delta R(T, \tau, \lambda)$ , where the  $\lambda$  is given by  $\lambda_{pr}$ .

### III. RESULTS AND DISCUSSIONS

We first outline the transient components, using  $\Delta R(T, \tau, 880\text{ nm})$  obtained at below, near, and above  $T_{CDW}$  [Fig. 1(b)]. In terms of the relaxation time, the transient  $\Delta R(\tau)$  is divided into three components: an instantaneous response ( $\approx 0.2\text{ ps}$ )  $\Delta R_{int}$  that is dominant in the metallic phase ( $T > T_{CDW}$ ), a subsequent exponential decay ( $\geq 0.5\text{ ps}$ )  $\Delta R_{gap}$  and a long-lasting offset  $\Delta R_{bg}$ . This combination has been widely observed in various quasi-1D and -two-dimensional CDW compounds,<sup>2,6</sup> and  $\Delta R_{int}$ ,  $\Delta R_{gap}$ , and  $\Delta R_{bg}$  can be associated with an intraband excitation/relaxation through a continuum, carrier recombination across the CDW gap, and relaxation via localized states within the gap, respectively.<sup>1,2</sup> The opening/closing of the gap is evidenced by the distinct changes in  $\Delta R_{gap}$  and  $\Delta R_{bg}$  with varying  $T$  across  $T_{CDW}$ . Below  $T_{CDW}$ ,  $\Delta R_{gap}$  exhibits a superposition of coherent oscillations, which can be attributed to collective excitations including lattice vibrations, and will be discussed in the latter part of the Rapid Communication.

The left-hand side of Fig. 2 shows 3D plots of  $\Delta R(T, \tau, \lambda)$  at  $T$  values ranging from  $T=10\text{ K}$  ( $\ll T_{CDW}$ ) to  $240\text{ K}$  ( $> T_{CDW}$ ). Although the amplitude of  $\Delta R$  varies significantly with  $\lambda$  and  $T$ , the transient  $\Delta R(\tau)$  consists roughly of the three components mentioned above, i.e.,  $\Delta R_{int}$ ,  $\Delta R_{gap}$ , and  $\Delta R_{bg}$ .

We now focus our attention on the cross-sectional spectra of  $\Delta R(\tau=0, 1, 20\text{ ps}, \lambda)$  shown on the right-hand side of Fig. 2, in which one can see the  $\Delta R$  resonances that allow a selection of coexisting CDW phase. In each spectrum, the difference between the gray [ $\Delta R(0\text{ ps}, \lambda)$ ] and red [ $\Delta R(1\text{ ps}, \lambda)$ ] curves connects the  $\Delta R_{int}$ , and the difference

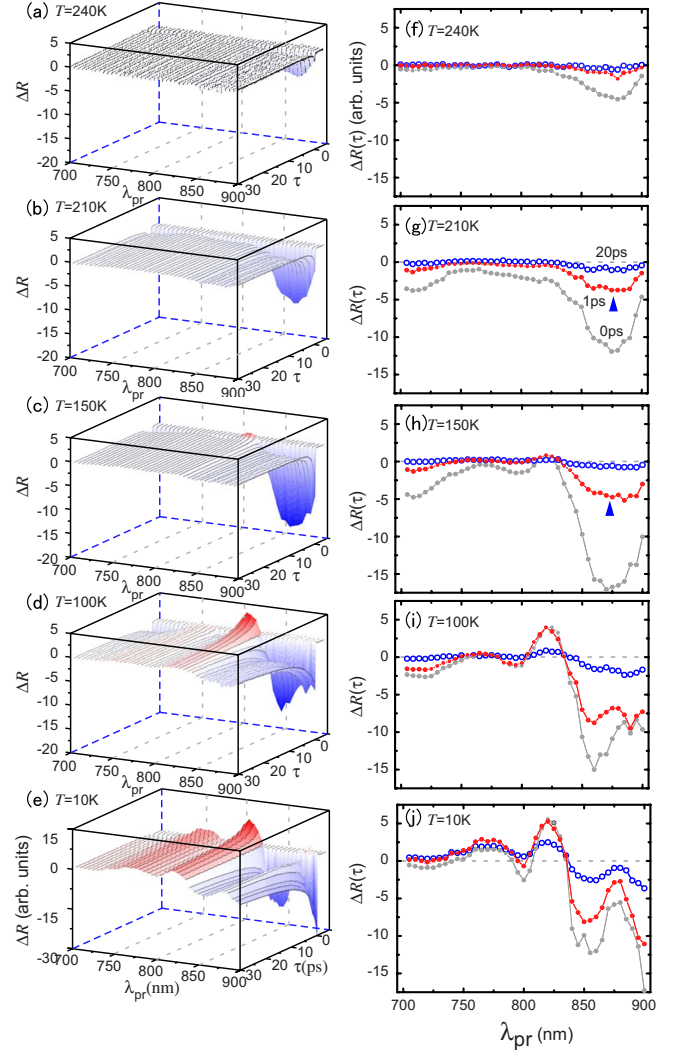


FIG. 2. (Color online) (a)–(e) 3D view of transient reflectivity changes,  $\Delta R(\tau, \lambda)$ , at various temperatures. (f)–(j) Transient spectral changes  $\Delta R(\lambda)$  at  $\tau=0$  (gray, solid circle), 1 (red, solid circle), and 20 ps (blue, open circle). The arrow indicates a negative peak whose shape and  $T$  dependence roughly match the changes of stationary reflectivity spectra.

between the red (solid circles) and blue [open circles,  $\Delta R(20\text{ ps}, \lambda)$ ] connects  $\Delta R_{gap}$  components. The blue (open circles) curve is almost identical to  $\Delta R_{bg}$ . Above  $T_{CDW}$ , only  $\Delta R_{int}$  exhibits distinct values and forms a single spectral peak (solid arrow) with a negative sign around  $\lambda=880\text{ nm}$ , which is located on the higher energy side of the  $R$  peak [see Fig. 1(a)]. When  $T$  is decreased below  $T_{CDW}$ , this peak becomes clear in both  $\Delta R_{int}$  and  $\Delta R_{gap}$ . In Figs. 2(b) and 2(g), the enhancement of  $\Delta R_{int}$  over the whole spectral region is observed, reflecting the  $ic$ CDW phase transition at  $T \approx T_{CDW}$ . When  $T$  is decreased further, the peak shifts to a shorter  $\lambda$  and forms several oscillatory resonances. At the lowest  $T$  ( $T=10\text{ K}$ ),  $\Delta R$  forms more than two oscillations within the observed spectral range.

The  $\Delta R(T)$  spectrum at  $\tau \approx 0$  can be associated with the change induced in the stationary  $R(T)$  spectra as the sample temperature is raised from  $T_b$  to  $T_a$ , where  $R(T_a)$  and  $R(T_b)$

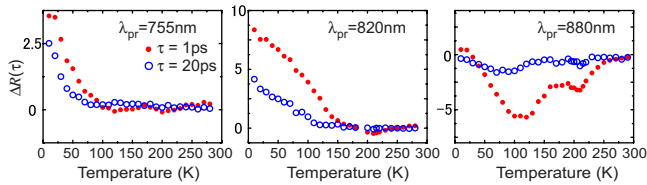


FIG. 3. (Color online) Temperature dependences of  $\Delta R$  [ $\tau=1$  (red, solid circle) and 20 ps (blue, open circle)] at various  $\lambda_{pr}$ .

reflect the optical transitions of hot and cold carriers, respectively.<sup>4</sup> In Fig. 1(a), the  $R$  peak slightly shifts to shorter  $\lambda$  with decreasing  $T$ . The  $\Delta R(T, \tau \approx 0) \equiv R(T_a) - R(T_b)$  thus produces a negative peak on the higher energy (shorter  $\lambda$ ) side of the  $R$  peak, which agrees with the  $T$ -dependence of the  $\Delta R$  peak in Fig. 2. The blueshift of  $R$  peak provides another positive  $\Delta R$  peak on the lower energy side, which is not visible in Fig. 2 because of the wavelength limit of the probe laser. The shorter  $\lambda$  shift is consistent with the optical transition from the gap state, where the resonance energy should be shifted by the amount of gap energy.<sup>22</sup> On the basis of this idea, additional oscillatory  $\Delta R(\lambda)$  resonances, which start to appear around 150 K and become significant below 100 K, suggest that the probe transition splits into several transitions with decreasing  $T$ . Note that the corresponding spectral changes should be included in the stationary  $R$  (Ref. 21) but could not be resolved clearly due to the low sensitivity compared to the pump-probe ( $\Delta R$ ) measurement. Furthermore, the intense broad  $R$  peak may obscure such additional tiny changes. In other words, the transient  $\Delta R$  with high sensitivity allows to emphasize the spectral changes associated with the phase ordering.

As mentioned in Sec. I, below  $T_{CDW}/2$ , the appearance of a new ordered phase has been suggested in various spectroscopic measurements.<sup>11–19</sup> For example, interlayer tunneling spectroscopy clearly indicates the existence of subgap states (amplitude soliton states) inside the CDW gap for NbSe<sub>3</sub> and TaS<sub>3</sub>.<sup>17</sup> Therefore the oscillatory resonances are associated with the optical transitions from the states formed by the commensurability. As is clearly seen in Figs. 2(e) and 2(j), the resonances superimpose on the negative peak, indicating the coexistence of two types of ground states. A similar result has been reported by Inagaki *et al.*, who used an angle-resolved synchrotron x-ray measurement to demonstrate that the  $ic$ - and  $c$ -CDWs coexist in the  $c$ CDW phase.<sup>19</sup>

When lowering the temperature below 100 K, the  $\Delta R$  spectrum itself does not show any remarkable changes except for the development of spectral oscillations whereas the angle-resolved x-ray measurement shows disappearance of the double peak structure below  $T=50$  K.<sup>19</sup> Moreover, in this temperature range, the dielectric response shows a glass transition.<sup>11,12</sup> In order to clarify the precise  $T$  dependence, the  $T$  dependences of  $\Delta R(\tau=1, 20$  ps) obtained at typical three  $\lambda_{pr}$  are shown in Fig. 3. The spectral changes at  $T=T_{CDW}$  and  $T_{CDW}/2$  are confirmed in  $\Delta R(1$  ps, 880 nm). Below 100 K,  $\Delta R(20$  ps)  $\approx \Delta R_{bg}$  starts to appear, and its magnitude increases with decreasing temperature at  $\lambda_{pr}=820$  and 755 nm. The upturn of  $\Delta R(20$  ps, 880 nm) with decreasing temperature results from the formation of the positive peak in the  $\Delta R$  spectrum. Because  $\Delta R_{bg}$  reflects

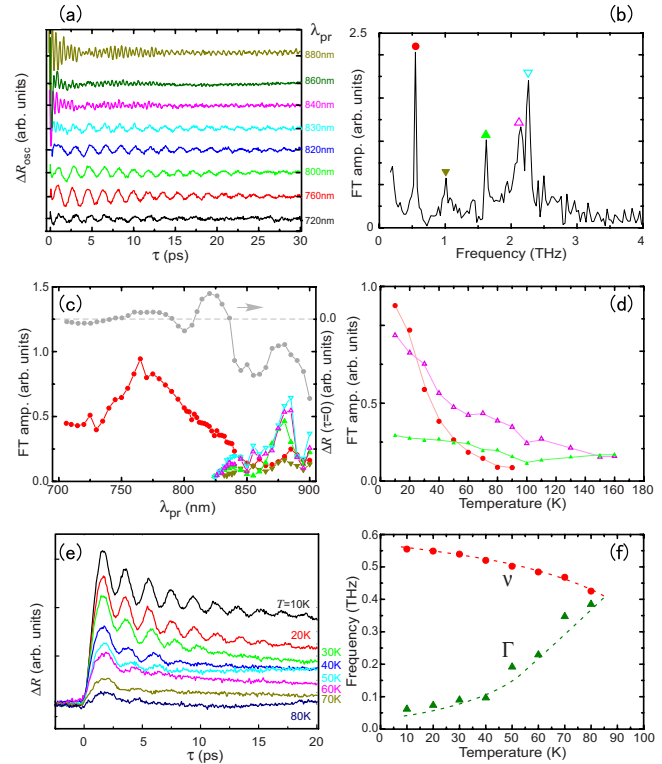


FIG. 4. (Color online) (a) Typical transient oscillation signals ( $\Delta R_{osc}$ ) obtained at various  $\lambda$ s at 10 K, where  $\Delta R_{osc}$  is evaluated by subtracting the exponential contributions from  $\Delta R$ . (b) A Fourier-transform (FT) spectrum obtained at  $\lambda=830$  nm at  $T=10$  K. Note that some of the high-frequency modes can also be identified in optical Raman spectra (Ref. 20). (c) Plots of magnitudes of the coherent oscillation modes at  $T=10$  K as a function of  $\lambda$ , where the magnitudes of individual modes are evaluated by the amplitudes of the FT spectral peaks. The symbols (colors) are defined in (b). For comparison, DR spectrum is also plotted on top. (d)  $T$  dependences of the typical three oscillation amplitudes. The lowest frequency mode disappears around  $T=100$  K due to a damped-overdamped transition of the oscillation. (e)  $\Delta R(\tau, 760$  nm) in the low-temperature range. A large oscillation corresponds to the lowest frequency mode. (f)  $T$  dependences of the frequency ( $\nu$ ) and damping constant ( $\Gamma$ ) of the lowest mode.

the relaxation via localized states within the gap, the increase of  $\Delta R_{bg}$  with decreasing the temperature is connected with a freezing of the dielectric response (glass transition at  $T \approx 40$  K).<sup>11,12</sup> This property also suggests the complete formation of the commensurate phase, which is consistent with the disappearance of the double peak structure observed in the angle-resolved x-ray measurement.<sup>19</sup>

We now examine the coherent oscillations ( $\Delta R_{osc}$ ) whose pronounced variations with both  $T$  and  $\lambda$  support the distinct selection of two types of CDW order. We plot the typical  $\Delta R_{osc}$  obtained at 10 K in Fig. 4(a), where one can clearly see a spectral variation; the high-frequency oscillation is dominant at  $\lambda \approx 880$  nm while  $\Delta R_{osc}(\lambda < 800$  nm) exhibits only one slow oscillation. The  $\Delta R_{osc}(\lambda \approx 830$  nm) corresponds to a crossover between the two regimes and its FT amplitude spectrum results in a number of sharp peaks [Fig. 4(b)]. This connection is more clearly defined in Fig.



4(c), where we plot the FT amplitudes of six typical modes labeled in Fig. 4(b) as a function of  $\lambda$ . For a comprehensive comparison, we also plot the  $\Delta R_{int}$  spectrum in the figure. The high-frequency modes produce a peak positioned around the  $\Delta R$  resonance of *ic*CDW while the low mode at 0.55 THz is significant in the shorter  $\lambda$ . The coexistence of these two different types of oscillation supports the coexistence of two types of optical transition. The correlations between the  $\Delta R_{osc}$  and  $\Delta R$  resonances are also evidenced by the  $T$  dependence of the oscillation mode amplitudes as summarized in Fig. 4(d), where the amplitude of the lowest mode (red circles) becomes small with increasing  $T$  and disappears around  $T=100$  K while the other high modes are still visible above  $T=100$  K and become small as  $T$  increases further [see Fig. 1(b) as a typical example]. At  $T\sim 200$  K ( $\approx T_{CDW}$ ), the high modes also vanish completely. The  $T$  dependences and the spectral correlation suggest that the coherent collective oscillations associated with the individual CDW ground states can be selectively excited.

Finally we consider the  $T$  dependences of the frequency and damping constant of the low-frequency mode [Fig. 4(e)] as summarized in Fig. 4(f). The frequency of the mode decreases from 0.55 to 0.4 THz as  $T$  increases from 10 to 80 K. The damping constant increases greatly along with the softening, and the oscillation finally becomes overdamped around 80 K. Similar  $T$ -dependent coherent oscillation was observed in quasi-1D  $K_{0.3}MoO_3$ , and was attributed to the CDW amplitude mode (AM) from the good correspondence

with Raman and neutron data.<sup>2</sup> Therefore, we associate the low-frequency oscillation with an AM mode of *o*-TaS<sub>3</sub>. The  $T$  dependence of the FT amplitude is in good agreement with that of  $\Delta R_{bg}$  described above, and thus associated with the glass transition of *o*-TaS<sub>3</sub>.

#### IV. CONCLUSION

In conclusion, we have studied the ultrafast carrier dynamics in a quasi-1D compound *o*-TaS<sub>3</sub> using a spectrally resolved pump-probe measurement. A distinct near-infrared resonance in this compound emphasizes the characteristic  $\Delta R$  associated with the CDW phase transition, and allows selective detection of multiple ground states. The  $T$ -dependent spectral changes of transient  $\Delta R$  and coherent oscillations indicate the coexistence of two types of CDW ordering at low temperature and clearly disentangle the individual phase transitions. We believe that our demonstration paves the way for the optical selection of the multiple phase order that plays an important role in various macroscopic quantum systems.

#### ACKNOWLEDGMENTS

This work was supported by the 21st century COE program ‘‘Topological Science and Technology,’’ MEXT, Japan. Y.T. acknowledges the Sumitomo foundation and the foundation for opto-science and technology.

- <sup>1</sup>V. V. Kabanov, J. Demsar, B. Podobnik, and D. Mihailovic, Phys. Rev. B **59**, 1497 (1999).
- <sup>2</sup>J. Demsar, K. Biljakovic, and D. Mihailovic, Phys. Rev. Lett. **83**, 800 (1999).
- <sup>3</sup>Y. Xu, M. Khafizov, L. Satrapinsky, P. Kus, A. Plecenik, and R. Sobolewski, Phys. Rev. Lett. **91**, 197004 (2003).
- <sup>4</sup>R. Kaindl, M. Woerner, T. Elsaesser, D. Smith, J. Ruan, G. Farnan, M. McCurry, and D. Walmsley, Science **287**, 470 (2000).
- <sup>5</sup>D. J. Hilton, R. P. Prasankumar, S. A. Trugman, A. J. Taylor, and R. D. Averitt, J. Phys. Soc. Jpn. **75**, 011006 (2006).
- <sup>6</sup>K. Shimatake, Y. Toda, and S. Tanda, Phys. Rev. B **75**, 115120 (2007).
- <sup>7</sup>Y. H. Liu, Y. Toda, K. Shimatake, N. Momono, M. Oda, and M. Ido, Phys. Rev. Lett. **101**, 137003 (2008).
- <sup>8</sup>T. Sambongi, M. Yamamoto, K. Tsutsumi, Y. Shiozaki, K. Yamaya, and Y. Abe, J. Phys. Soc. Jpn. **42**, 1421 (1977).
- <sup>9</sup>F. Ya. Nad’ and P. Monceau, Phys. Rev. B **46**, 7413 (1992).
- <sup>10</sup>J. Nakahara, T. Taguchi, T. Arai, and M. Ido, J. Phys. Soc. Jpn. **54**, 2741 (1985).
- <sup>11</sup>F. Nad’ and P. Monceau, Solid State Commun. **87**, 13 (1993); Phys. Rev. B **51**, 2052 (1995).
- <sup>12</sup>D. Starešinić, K. Biljaković, W. Brütting, K. Hosseini, P. Monceau, H. Berger, and F. Levy, Phys. Rev. B **65**, 165109 (2002).

- <sup>13</sup>R. C. Rai and J. W. Brill, Phys. Rev. B **70**, 235126 (2004).
- <sup>14</sup>K. Biljaković, M. Miljak, D. Starešinić, J. C. Lasjaunias, P. Monceau, H. Berger, and F. Levy, Europhys. Lett. **62**, 554 (2003).
- <sup>15</sup>J. Dumas, J. C. Lasjaunias, K. Biljakovic, M. Miljak, H. Berger, and F. Levy, Solid State Commun. **132**, 661 (2004).
- <sup>16</sup>S. L. Herr, G. Minton, and J. W. Brill, Phys. Rev. B **33**, 8851 (1986).
- <sup>17</sup>Y. I. Latyshev, P. Monceau, S. Brazovskii, A. P. Orlov, and T. Fournier, Phys. Rev. Lett. **96**, 116402 (2006).
- <sup>18</sup>S. V. Zaitsev-Zotov and V. E. Minakova, Phys. Rev. Lett. **97**, 266404 (2006).
- <sup>19</sup>K. Inagaki, M. Tsubota, K. Ichimura, S. Tanda, K. Yamamoto, N. Hanasaki, Y. Nogami, N. Ikeda, T. Ito, and H. Toyokawa, Phys. Soc. Jpn. **77**, 093708 (2008); Physica B **404**, 396 (2009).
- <sup>20</sup>S. Sugai, Phys. Rev. B **29**, 953 (1984).
- <sup>21</sup>Indeed, the authors in Ref. 10 found the appearance of the side peaks in  $R$  resonance as decreasing  $T$ . This is also supported by a remarkable shrinkage of the peak width at 10 K in Fig. 1(a).
- <sup>22</sup>If we choose the  $R$  resonance ( $\lambda\sim 905$  nm) as the initial position for optical transition above  $T_{CDW}$ , the shift of the peak ( $\lambda\sim 870$  nm at 170 K) is evaluated to be  $\sim 55$  meV ( $445$  cm<sup>-1</sup>). Although our estimation includes ambiguity, this value is consistent with  $\Delta$  in the previous reports (Refs. 16 and 17).